Chapter 10
Utility of OCT for Detection or Monitoring of Glaucoma in Myopic Eyes

Atilla Bayer and Kouros Nouri-Mahdavi

10.1 Introduction

Myopia is one of the most common ocular conditions worldwide and its association with glaucoma is well recognized [1–4]. Myopia has been increasing at a rapid rate in the younger population, and a dramatic rise in the prevalence of myopia is expected as this population ages [2]. It is accompanied by various degenerative changes in the posterior segment structures of the eye including the sclera, optic nerve head (ONH), choroid, Bruch's membrane, retinal pigment epithelium (RPE), and neurosensory retina. Thorough understanding of anatomic changes in the ONH and retinal nerve fiber layer (RNFL) is important especially considering the fact that myopic eyes are 2–3 times more likely to develop glaucoma compared to non-myopic eyes [3, 5]. In a recent study by Shim and associates, OAG developed earlier in participants with high myopia than in others [1]. There was a high prevalence of OAG in participants with high myopia, even in those 19–29 years of age.

Optical coherence tomography (OCT) has enabled recognition of morphological changes in glaucoma, which was not previously possible on clinical examination [6]. OCT studies of altered biometry and topography of the ONH, retina and choroid has allowed evaluation of their relationship with demographic factors, visual function, and fundoscopic findings in myopia [7]. As the normative databases of current OCT devices largely comprise data collected from normal eyes with no or low degrees of myopia, the deviation maps or classification charts provided by such devices are likely to be inaccurate in highly myopic eyes. Volume scans acquired with most commercial OCT instruments have a depth of focus of about 2 mm. The posterior eye

A. Bayer (✉)
Department of Glaucoma, Dünyagöz Eye Hospital, Ankara, Turkey

K. Nouri-Mahdavi
Stein Eye Institute, University of California Los Angeles, Los Angeles, CA, USA
e-mail: nouri-mahdavi@jsei.ucla.edu

A. Akman et al. (eds.), *Optical Coherence Tomography in Glaucoma*,
https://doi.org/10.1007/978-3-319-94905-5_10

wall of a highly myopic eye has sometimes curvatures that exceed this limit. Other characteristics of myopic eyes mentioned above also create difficulties on OCT imaging. This chapter provides updated information on the current uses, limits, and keypoints of OCT imaging in myopic eyes with suspected or definitive glaucoma.

10.2 Ocular Features of Myopia and Implications in Glaucoma

10.2.1 Challenges in Detecting and Managing Glaucoma

Glaucoma is assessed clinically mostly by evaluating changes in the ONH or in the visual field (VF). Myopia may affect these measurements. Uneven expansion of the posterior globe wall leading to tilting of the disc and subsequent oval shape of the disc, shallow enlarged cupping, peripapillary atrophy (PPA), and poor media are some of the characteristics of myopic eyes that make disc evaluation challenging (Fig. 10.1) [5, 6]. Degenerative changes in the peripapillary region in degenerative myopia could lead to VF defects that can mimic those observed in glaucoma.

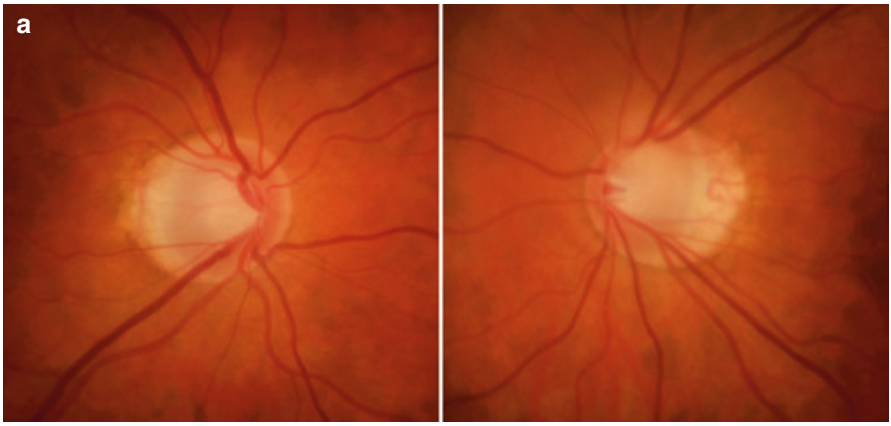

Fig. 10.1 (**a**) Optic disc photographs of a female patient with moderate to high myopia (−5.00 D, SE) and suspected of glaucoma. Suspicious looking tilted large optic discs can be observed with peripapillary atrophy (PPA) and enlarged cups bilaterally. (**b**) Visual field tests are classified as "within normal limits" bilaterally. (**c**) Spectralis OCT baseline retinal nerve fiber layer (RNFL) tests in year 2011 were classified as "borderline" and "outside normal limits" in the right and left eyes, respectively. However, the findings are due to displaced RNFL peaks and the RNFL Change Report is stable in both eyes over 5 years of follow-up. (**d**) In the Posterior Pole Asymmetry Analysis tests, there is suspected thinning in the baseline hemisphere asymmetry charts but both eyes are stable during the 5 years of follow up as indicated back the lack or regions of thinning retinal thickness that would be flagged in red on the right bottom subtraction image

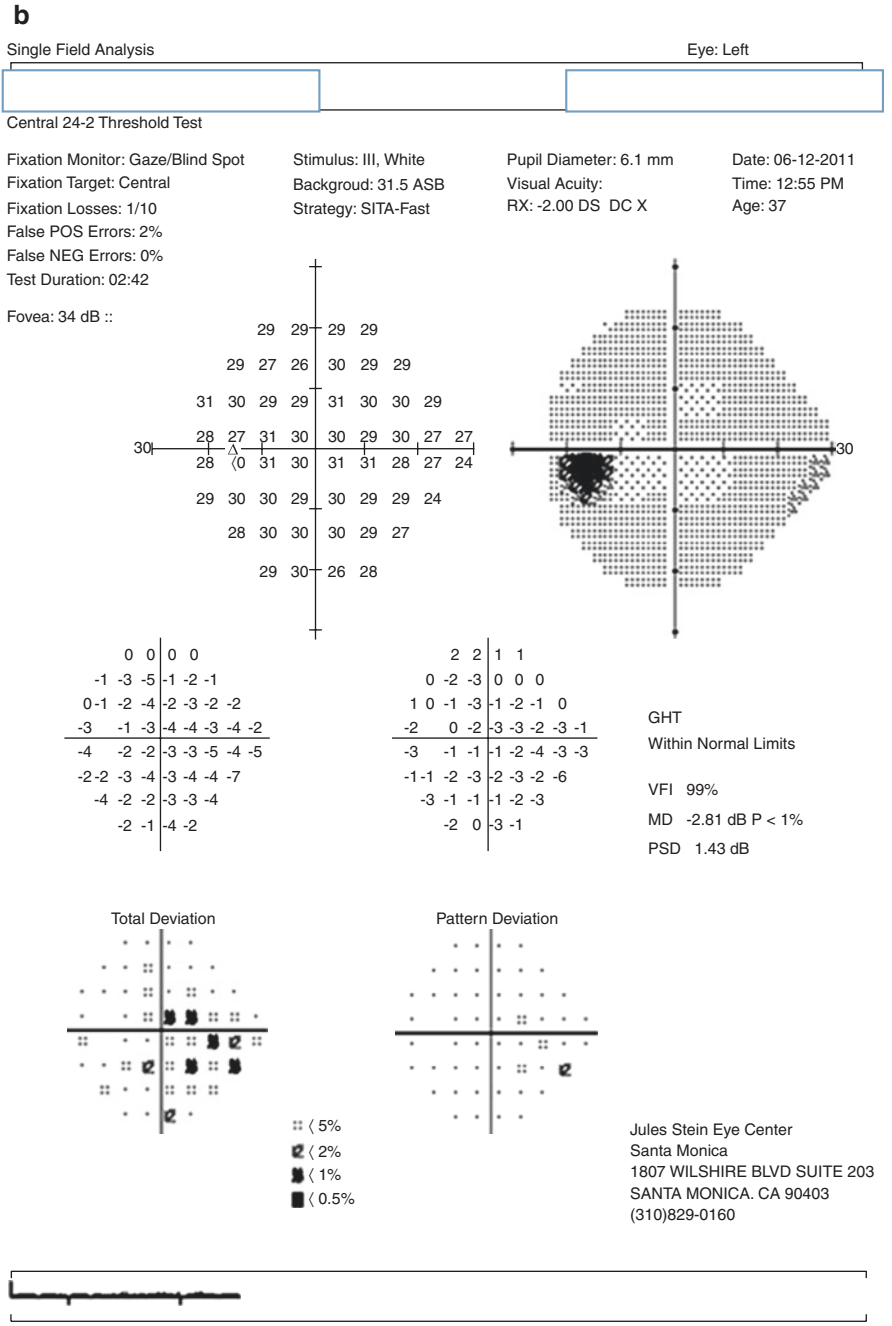

Fig. 10.1 (continued)

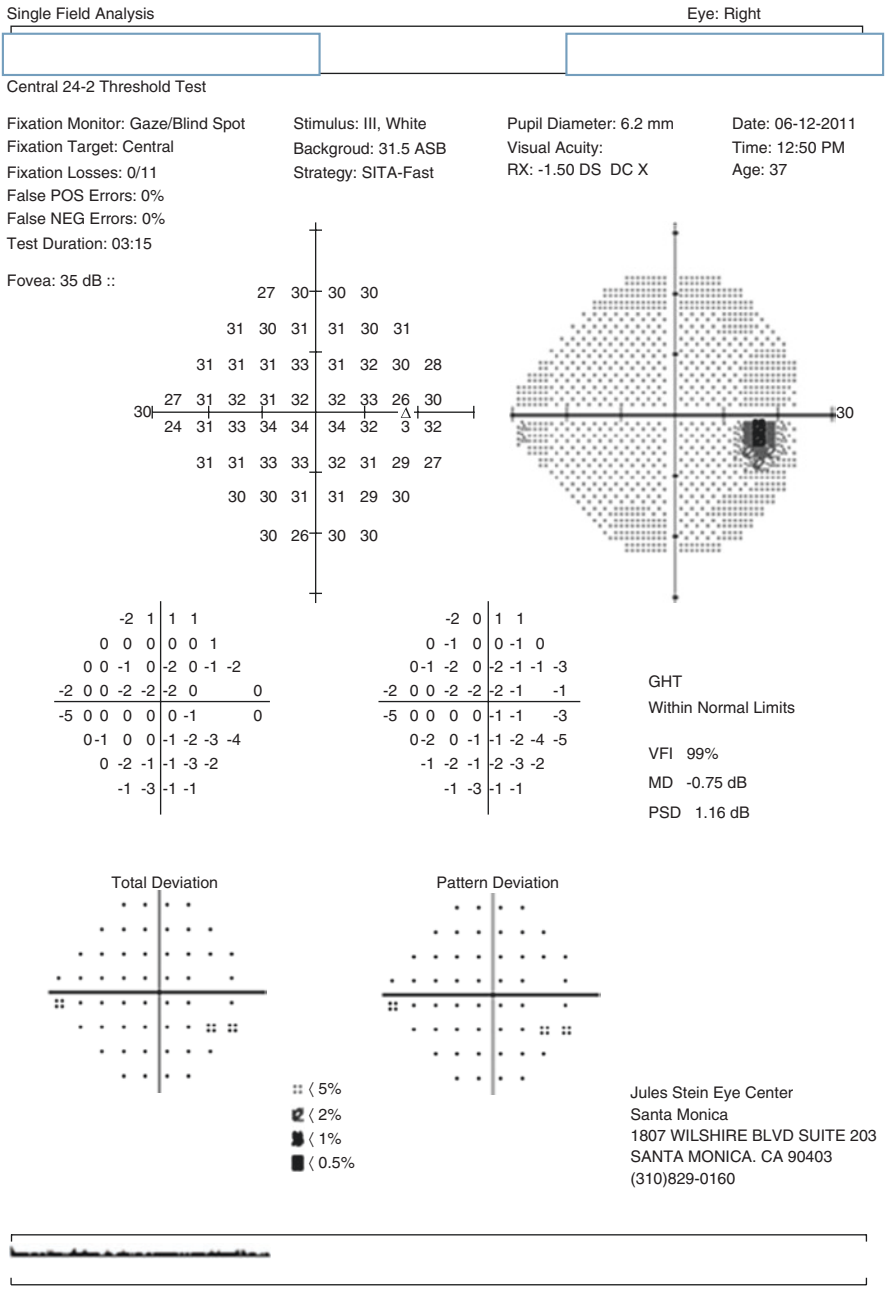

Fig. 10.1 (continued)

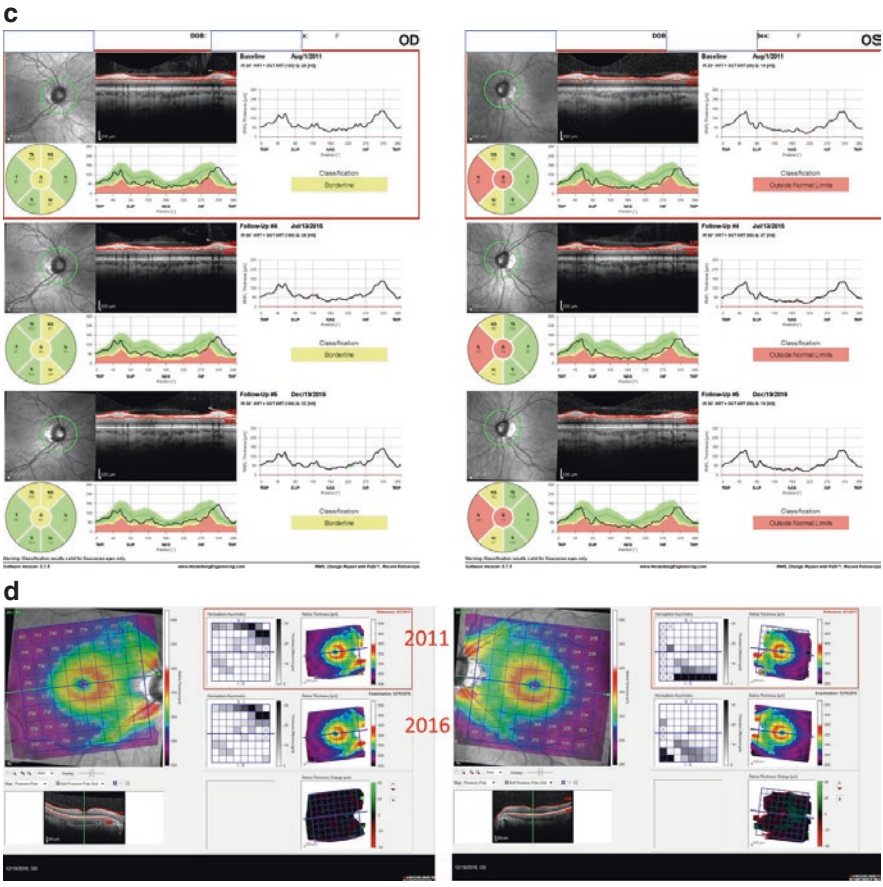

Fig. 10.1 (continued)

Thinning of the eyewall layers in myopia changes the scleral rigidity. Lower corneal hysteresis has been reported as another characteristic of myopic eyes affecting IOP measurements [8–10]. These characteristics of myopic eyes can make an accurate glaucoma diagnosis challenging, since there is no proven biomarker for the disease. Preventive treatment can be bothersome and expensive and have potential side effects. Given that a correct diagnosis before VF damage emerges is difficult at best, some myopes are probably overtreated while others with glaucoma are being undertreated or go completely untreated.

10.2.2 Optic Nerve Head Changes

Detecting glaucoma in eyes with low to moderate myopia is not more challenging than emmetropic eyes, since the appearance of the ONH is more or less similar [11]. In high axial myopia, including the highly myopic form of primary open angle glaucoma, the eyewall stretches and the axial length increases. During this process, the ONH is pulled towards the temporal direction, which eventually results in an optic disc with a temporally tilted appearance with elevation of the nasal disc margin and temporal flattening [11–13]. Jonas and associates recently reviewed the histological changes of high axial myopia [14]. In their study, scleral thinning started at or behind the equator with maximal thinning in the posterior pole. They also reported presence of an elongated scleral flange (defined as the canal between the optic nerve border and the point where dura mater merges with the sclera) and stretching and thinning of the lamina cribrosa with decreased distance between the retrobulbar cerebrospinal fluid space with the IOP compartment. Morgan and associates found that the pressure difference between the intraocular and retrobulbar spaces was distributed over a shorter length, resulting in steeper pressure gradient across the lamina cribrosa [15]. Development of large pores in lamina cribrosa has been reported as characteristic of eyes with primary open angle glaucoma [16].

Although a tilted disc appearance refers to the ONH being rotated around the vertical axis from a two-dimensional fundoscopic view, tilting of the disc can occur along horizontal or oblique axes (Fig. 10.2). The degree of the ONH tilt is estimated by the disc 'ovality' index, which is measured as the ratio of the longest to shortest

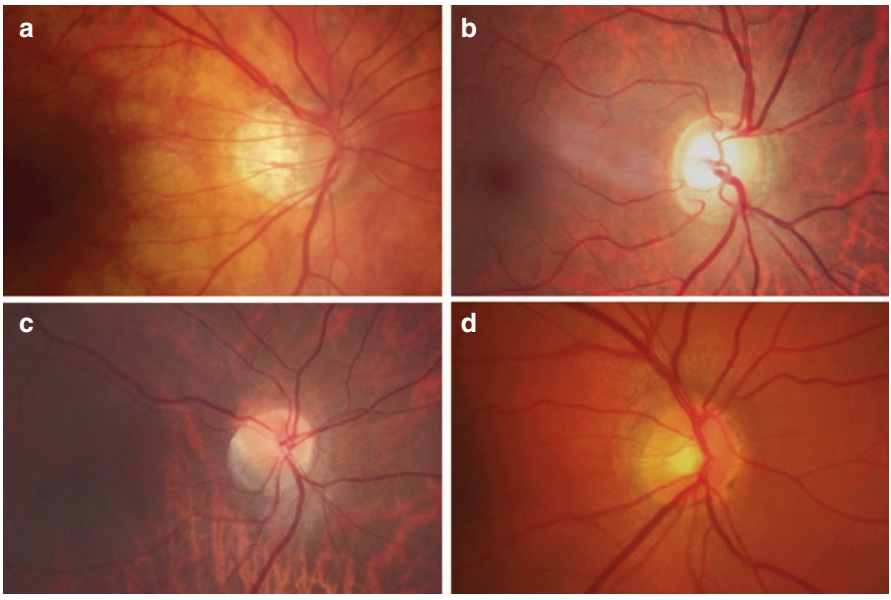

Fig. 10.2 Examples of tilted discs; (**a**) temporal tilt, (**b**) nasal tilt, also called disc dysversion, (**c**) inferotemporal tilt, (**d**) superotemporal tilt

diameters of the disc. On the other hand, the index of tilt is defined as the ratio of the shortest diameter to the longest diameter [17]. The course of ONH vessels also changes in tilted discs. The second geometric variable in the optic discs is the rotation about the sagittal axis of the ONH. This is defined as ONH torsion. However, disc torsion is now considered as tilting of the disc occurring along an oblique axis.

In a morphometric study conducted by Jonas and associates, optic discs of highly myopic eyes (>−8.0 diopters) were found to be significantly larger and shaped more oval than those of non-highly myopic eyes [12]. In another clinical observational study, ONH area was significantly larger in a subset of highly myopic eyes (>−8.0 diopters) [18]. The optic disc cup can also be remarkably shallow in myopic eyes.

10.2.3 Peripapillary Atrophy

Peripapillary atrophy, has classically been divided into a peripheral α-zone, and a central β-zone based on clinical findings. The latter has been known to be associated with glaucomatous optic neuropathy and myopia. The α-zone is characterized by irregular hypopigmentation and hyperpigmentation of the RPE and slight thinning of the choroidal tissues. The hallmark of β-zone is a complete loss of the RPE, marked atrophy of the photoreceptor layer and the choriocapillaris, clear visibility of large choroidal vessels and sclera. It is marked by a sharp boundary along the adjacent α-zone and abuts the peripapillary scleral ring [19, 20] (Fig. 10.3). Recent histological and clinical investigations revealed that the peripapillary region in highly myopic eyes showed additional features. In some myopic eyes, between the β-zone and the clinical disc margin, there is an area lacking the Bruch's membrane called the γ-zone [21]. The γ-zone has traditionally been recognized as the myopic temporal crescent or conus [22, 23]. It is defined as a whitish area temporal to the

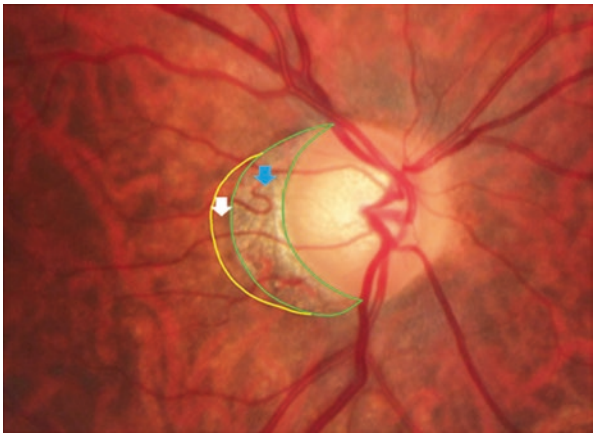

Fig. 10.3 The two zones of peripapillary atrophy defined clinically as the central β-zone (blue arrowhead) and a peripheral α-zone (white arrowhead)

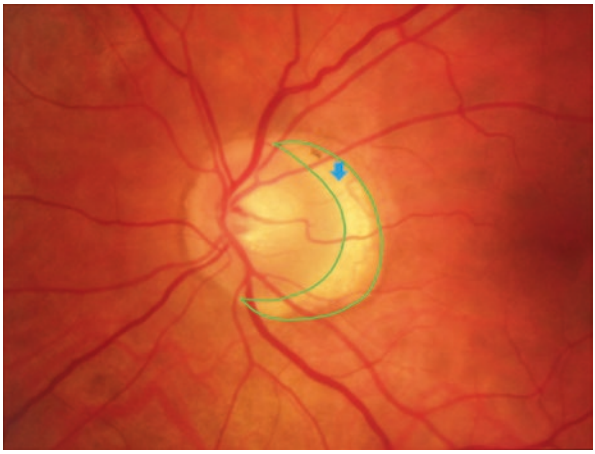

Fig. 10.4 Peripapillary γ-zone in a myopic eye (blue arrowhead)

disc margin without underlying choriocapillaris vessels and without any signs of RPE (Fig. 10.4). This zone of PPA must be differentiated from the β-zone which serves as a marker of glaucomatous disease and progression [21, 24].

10.2.4 The Macular Area and Posterior Pole Changes

Changes in the posterior wall and macular area of the eye may affect clinical evaluation of the retina especially in highly myopic cases. These changes can be summarized as posterior precortical vitreous pockets, precursor changes of posterior vitreous detachment, retinoschisis, peripapillary intrachoroidal cavitation, dome-shaped macula, and changes in the inner curvature of the sclera [25]. Fortunately, most of these changes can be diagnosed with OCT imaging. Details of these changes are outside the scope of this chapter. A few examples of changes that might affect detection of glaucoma are shown in Fig. 10.5.

10.3 OCT Findings in Myopia

10.3.1 The Optic Nerve Head

The anatomic changes in the ONH and surrounding structures of eyes in high myopia have been identified in vivo with OCT imaging. The angle of ONH tilting can be measured with OCT [26]. Other features of glaucomatous optic neuropathy that can be observed on OCT imaging include, enlargement of laminar pores (Fig. 10.6), dehiscence of the lamina cribrosa (seen as an acquired pit of the ONH in extreme cases), expansion of the dural attachment posteriorly with enlargement of the subarachnoid

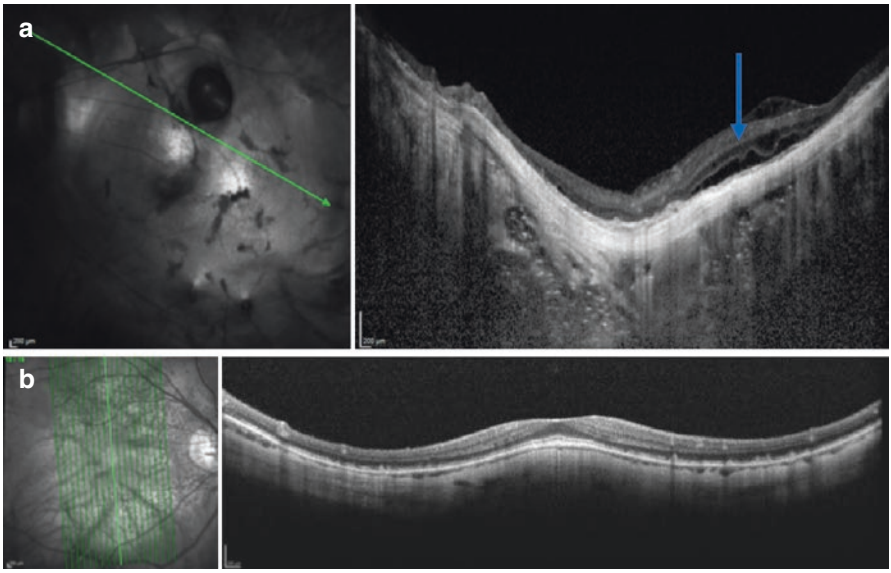

Fig. 10.5 (**a**) Posterior pole optical coherence tomography scan of a highly myopic eye with an axial length of 30.84 mm. Note that sclera is bowed posteriorly (top right, posterior staphyloma). The hyporeflective space (blue arrow) represents an area of retinoschisis, another finding observed in highly myopic eyes, which may interfere with glaucoma evaluation. (**b**) In some highly myopic eyes, convexity of the posterior staphyloma causes inward bulge of the macula, which is known as dome-shaped macula

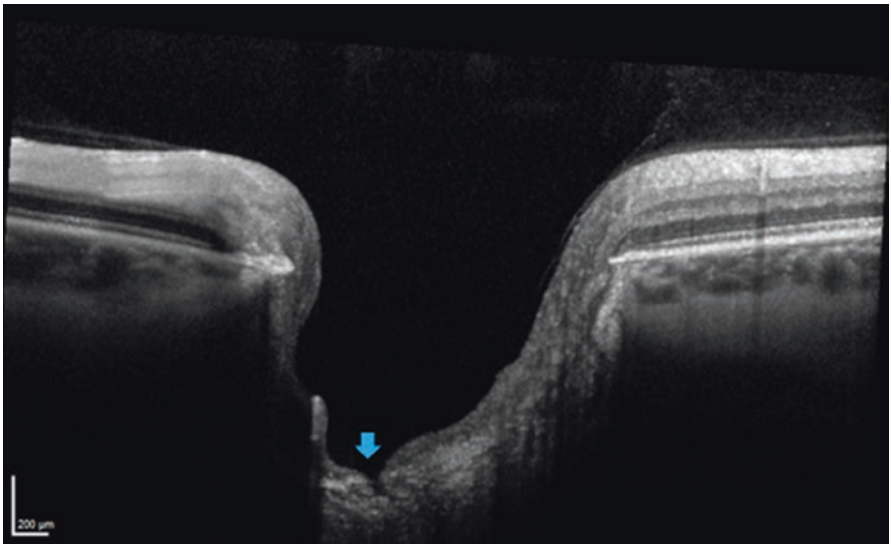

Fig. 10.6 Optical coherence tomography imaging of an enlarged laminar pore in a myopic eye (blue arrowhead)

space immediately behind the sclera and expansion of the circle of Zinn-Haller, with potentially compromised circulation of the prelaminar portion of the ONH [27].

Minimum rim width analysis with Glaucoma Module Premium Edition (GMPE) software of Spectralis OCT (Heidelberg Engineering Inc., Heidelberg, Germany) device may be helpful in myopic eyes when PPA or tilted ONH pose challenges to RNFL measurement.

10.3.2 The Retinal Nerve Fiber Layer

There are various sources of error with RNFL measurement in myopic eyes. These can be summarized as temporal displacement of RGC axons and blood vessels and torsional changes in the RNFL topography, problems with correct centering of the measurement circle on a myopic disc, variable focusing effect caused by tilting of the ONH, magnification issues related to myopic refraction, and segmentation errors. Peripapillary retinoschisis is also observed more frequently in myopic eyes.

Leung and associates measured the angle between the temporal superior and temporal inferior RNFL bundles on Cirrus HD-OCT images, and reported a reduction of this angle with increasing axial length [7]. As the axial length increases, the retina is dragged temporally and the RGC axons are compressed against the bundles originating from the opposite hemisphere temporal to the disc. This effect results in the thickening of the RNFL in the temporal quadrant and its thinning in the other quadrants especially nasally [28]. Temporal displacement of the vessels and RNFL peaks is typically observed in this scenario (Figs. 10.7 and 10.8).

Most of the current OCT devices automatically identify the optic disc or BMO centroid and center the calculation or scan circle on this centroid. Presence of a myopic tilted optic disc can make it challenging to determine the BMO centroid, therefore, confounding peripapillary RNFL analysis with OCT. For example, nasal displacement of the calculation circle causes thickening of the RNFL in the temporal region and decreases RNFL thickness in the other regions. In eyes with myopic tilted discs, the clinician should check the RNFL profile as well as the raw data and look for artifacts or other imaging issues, such as data being cut off due to marked height difference along the peripapillary the retina on the circular tomogram (Fig. 10.9). Raw images of the circular tomogram may also provide hints on the magnitude and axis of ONH tilt.

Location of the main temporal superior and inferior blood vessels is correlated with the RNFL thickness profile. In patients with ONH torsion, direction of torsion influences the location of blood vessels and peripapillary RNFL thickness, whereas the macular sectoral ganglion cell/inner plexiform layers (GCIPL) thickness is not affected [29]. Thickening of the temporal RNFL with temporal shifting of the superior peak in eyes with temporal (counterclockwise) ONH torsion can lead to interpretation errors because OCT devices provide sectorial analysis of the peripapillary RNFL based on their normative database. In this situation, ganglion cell or posterior pole analysis algorithms would be more helpful.

The average RNFL thickness may be affected by magnification of the ocular optical system, especially when myopia exceeds −4.0 diopters (D) [28, 30]. Current OCT

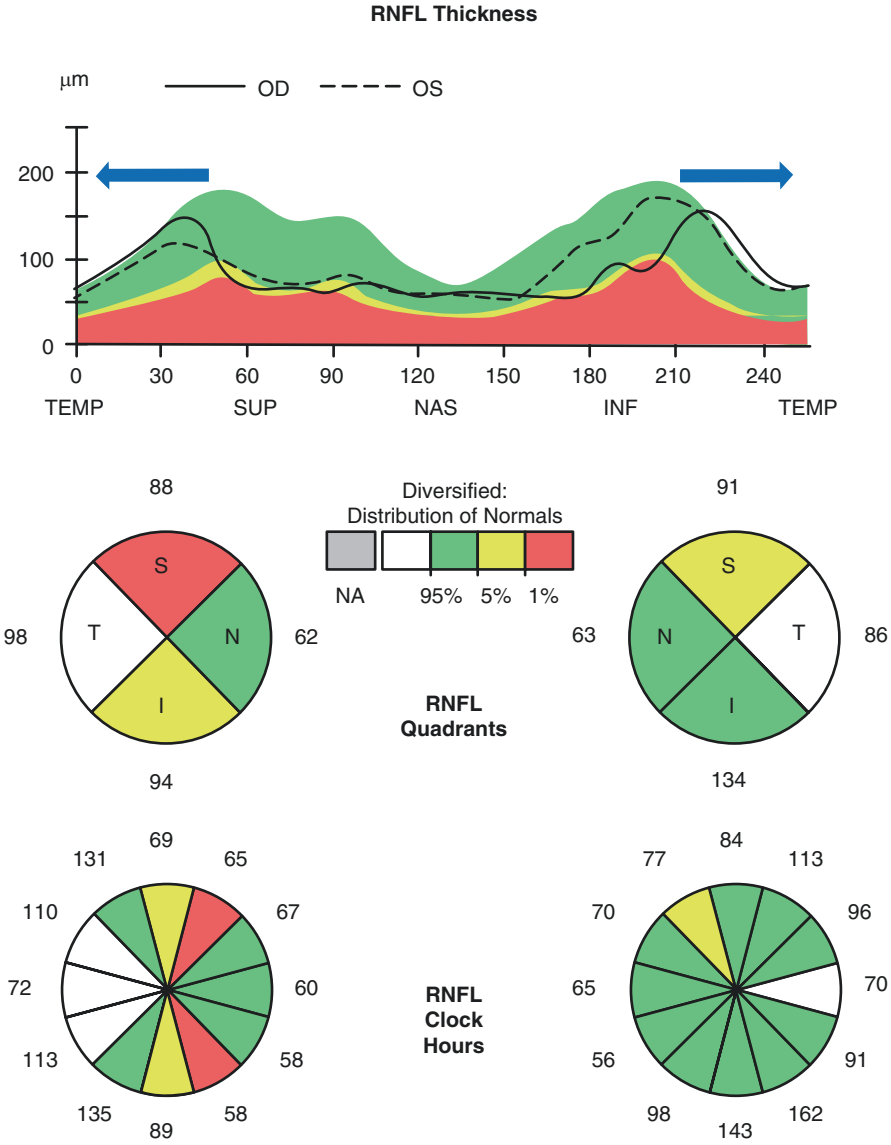

Fig. 10.7 Retinal nerve fiber layer (RNFL) analysis by Cirrus HD-OCT shows abnormally reduced thickness in superior and inferior sectors of the right eye and superior quadrant of the left eye of a myopic young patient suspected of glaucoma. The RNFL peaks on the thickness plots are temporally displaced in both eyes (blue arrows) leading to thickening of the RNFL (>95th percentile) in the temporal quadrants and apparent thinning superiorly in both eyes and inferiorly in the right eye

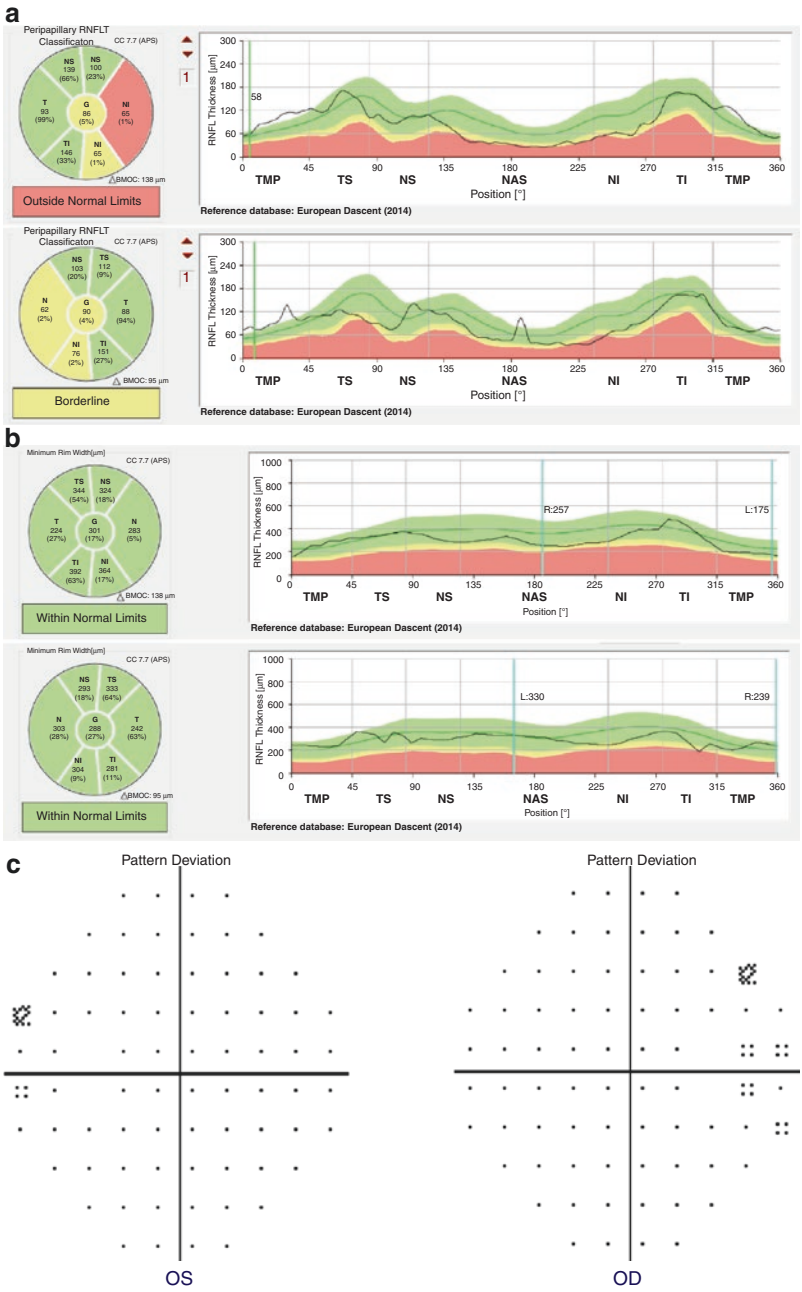

Fig. 10.8 This glaucoma suspect patient had myopia of −9 diopters (D) and −8.50 D in the right and left eyes, respectively. (**a**) Retinal nerve fiber layer (RNFL) thickness plots and classification charts showed thinning in the nasal sectors of both eyes with classification of 'outside normal limits' in the right eye, and borderline in the left eye based on sectoral analyses. (**b**) Minimum rim width analysis revealed measurements within normal limits in all sectors for both eyes. (**c**) Central 24-2 visual field tests were classified as within normal limits in both eyes

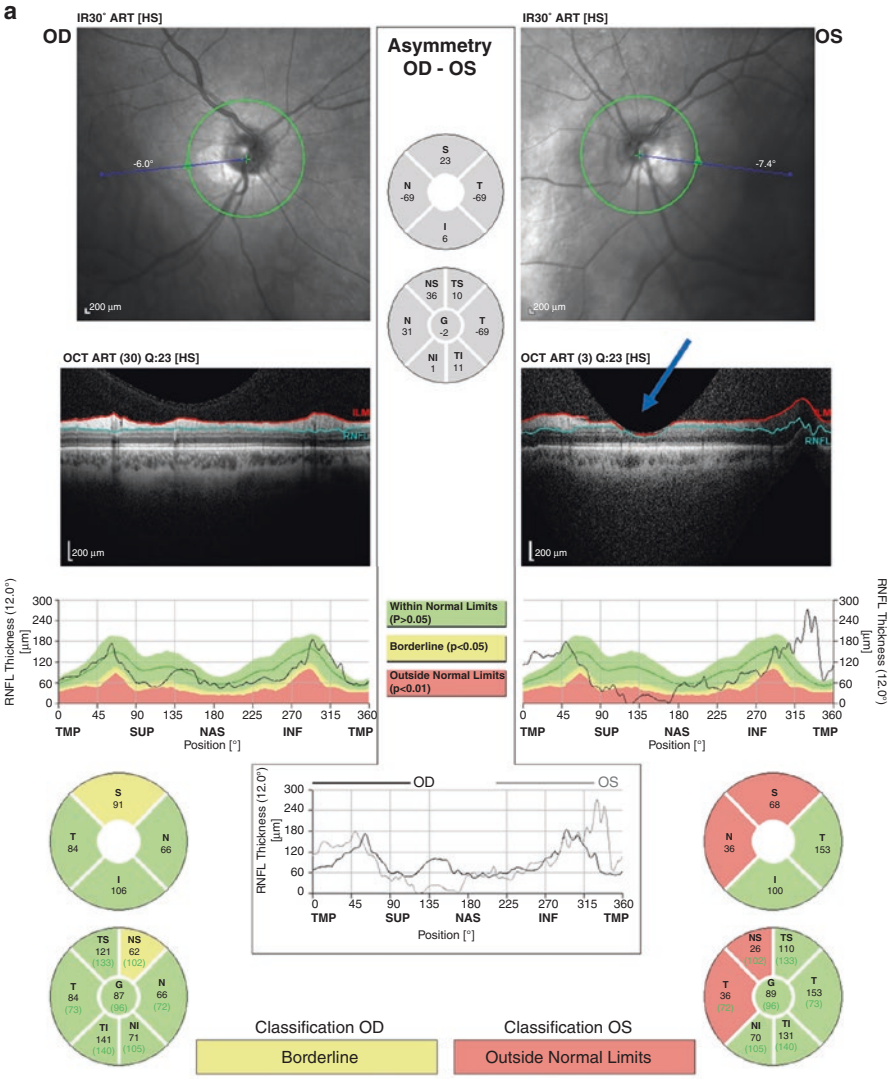

Fig. 10.9 (**a**) Spectralis optical coherence tomography (OCT) retinal nerve fiber layer (RNFL) printout of a patient with high myopia of −10.00 diopters spherical equivalent in both eyes, where classification was borderline in the right eye and outside normal limits in the left eye. When the RNFL profile of the left eye is carefully reviewed, one can see a crescent shaped defect in the retinal layers in the nasal superior area (see blue arrow). There is also artefactual thickening in the inferior temporal area; the likely cause is that because of the extreme curvature, the RNFL thickness is not measured perpendicularly. Classification is outside normal limits in the superior and nasal quadrants. (**b**) When the raw data is checked, one can see that the patient has inferotemporally tilted optic nerve head and the apex of the RNFL profile is out of the scanning zone, i.e., the difference between the retinal surface peak and trough almost exceeds the 2-mm depth of focus of the OCT device. (**c**) The test was repeated taking care that all the RNFL profile was fit within the scanning zone; the OCT classification is now within normal limits in the superior and nasal quadrants, although borderline thinning is present in the nasal superior sector, which is symmetrical in both eyes. (**d**) Raw image after the second test where RNFL profile is fit within the scanning zone

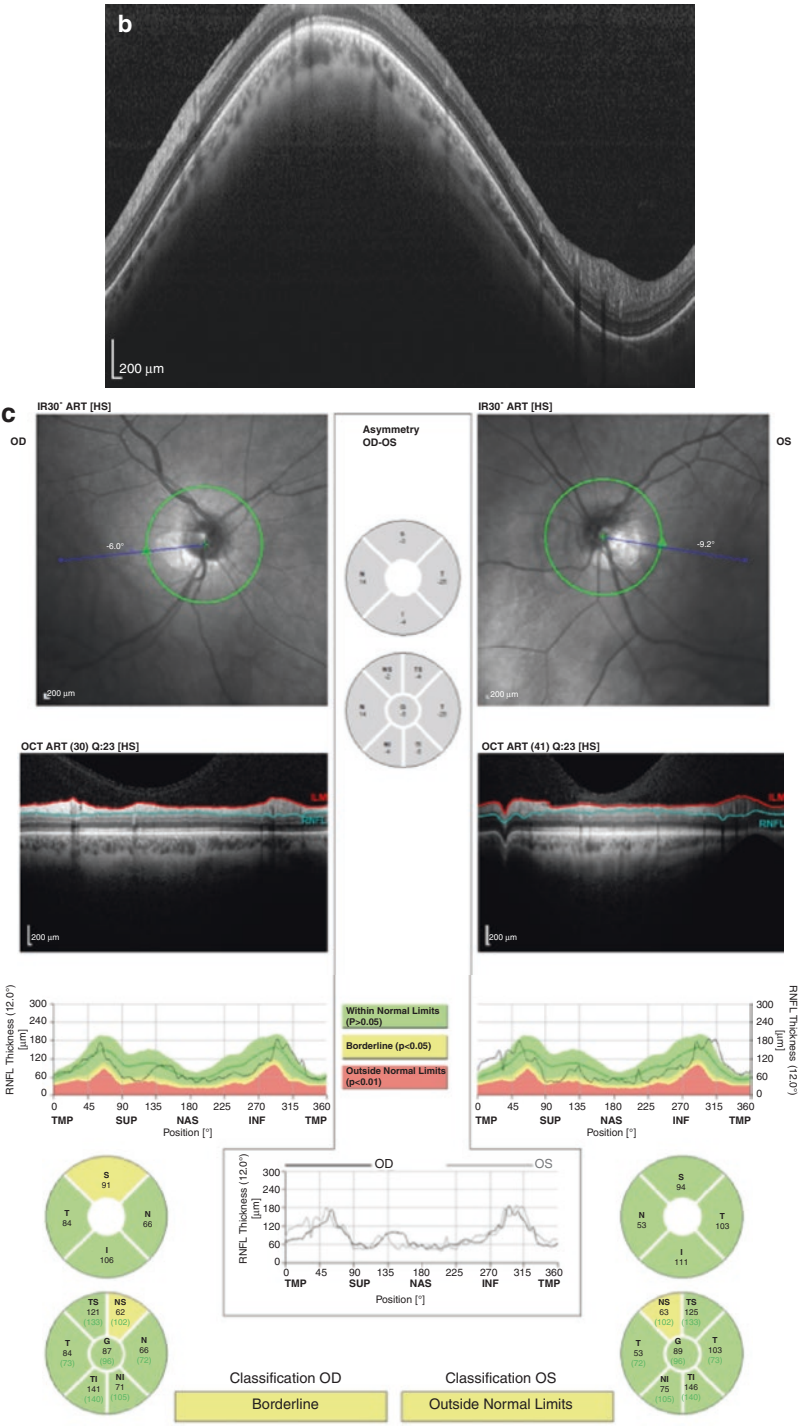

Fig. 10.9 (continued)

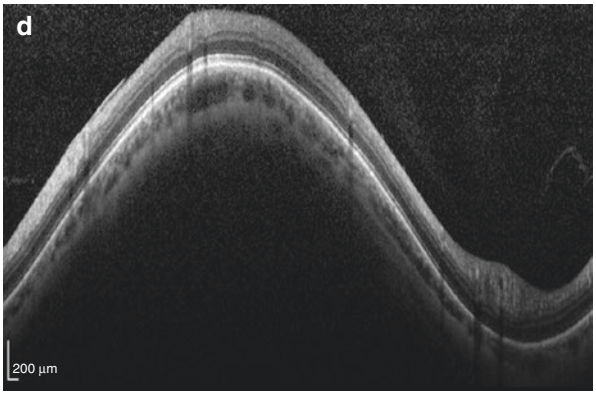

Fig. 10.9 (continued)

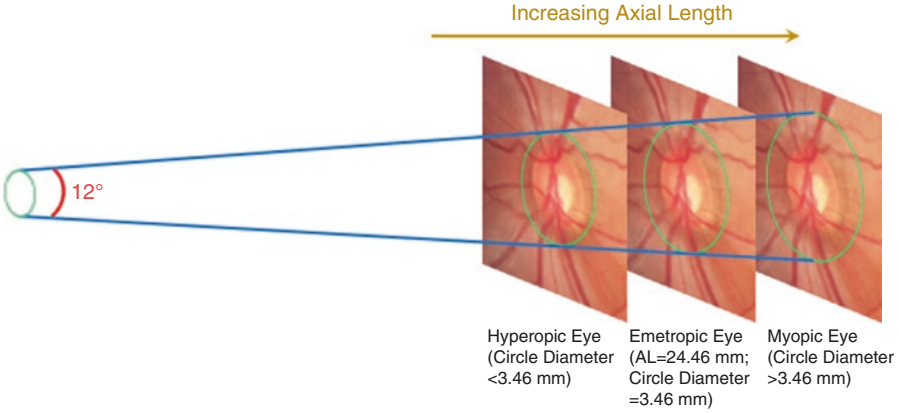

Fig. 10.10 Effect of axial length (AL) on the scan circle diameter. Scan circle is 3.46 mm in diameter in an emmetropic eye with average AL. Scan circle diameter directly affects the RNFL thickness measurements resulting in thinner measurements in a longer eye and thicker ones in a shorter eye

devices have been set to measure RNFL thickness at a fixed angular distance (approximately 12°) centered on the optic disc. However, the magnification effect of the eye is known to impact the actual size and hence, location, of the scan circle on the peripapillary retina [31]. The SD-OCT measurements are not thoroughly corrected for the magnification of the ocular optical system. Some devices such as Spectralis OCT require the corneal curvatures to be entered into the system before scanning. The additional focusing mechanism of the OCT devices also partially compensates for the axial length of the eye. A longer eye will result in a larger measurement circle diameter, thereby measuring the RNFL at a farther distance from the optic disc or BMO centroid. The reverse would apply to small eyes [32] (Fig. 10.10). Measurement circle's standard diameter of 3.46 mm in an emmetropic eye (considered as an eye with an axial length of 24.46 mm in Cirrus HD-OCT) decreases to 2.78 mm in a 20 mm long eye and increases to 4.00 mm in a 28 mm long eye [33].

In some myopic eyes, the automatic segmentation algorithms cannot accurately measure the RNFL thickness most commonly due to a larger area of PPA. In these cases, the lack of contrast between the RNFL and the remaining eyewall layers (typically only sclera) causes erroneous measurements. This is another issue that creates difficulty in the evaluation of glaucoma patients with high myopia [28]. Larger scan circles (4.1 and 4.7 mm in diameter) are available on the GMPE software of Spectralis, which may circumvent this issue.

To avoid misdiagnosis and to improve the sensitivity and specificity of glaucoma detection by OCT, a separate normative RNFL profile for myopic eyes is needed. The implementation of a myopic normative database in OCT instruments would potentially allow more precise interpretation of OCT printouts when used in myopic eyes. Recently, Seol and associates reported that the diagnostic ability of OCT significantly improved for detection of glaucoma in myopic eyes after incorporation of a customized myopic normative database into Cirrus HD-OCT (Fig. 10.11) [34].

In eyes with peripapillary retinoschisis, a transient increase in the RNFL thickness measurements is commonly observed (Fig. 10.12); after the resolution of retinoschisis, the RNFL thickness decreases remarkably. We propose that clinicians should examine the thickness maps as well as the raw OCT images in order to rule out retinoschisis so as not to overestimate the RNFL thickness or misinterpret the resolution of retinoschisis as a rapid structural progression. An area with supernormal RNFL thickness is oftentimes a clue to the presence of schisis areas. The schisis cavity can occasionally be observed as a darker, more or less localized, area on the *en face* IR images. More studies on this topic are needed to clarify whether a collapse of the schisis cavity represents a significant event in the course of RNFL deterioration.

10.3.3 Peripapillary Atrophy

In the infrared (IR) images, ONH can be surrounded by an area of hyper-reflectance, more commonly visible in the temporal area. This area corresponds to the PPA observed on fundus exam and is a possible source of OCT artifacts in myopic eyes as mentioned above. Proper identification of PPA zones is important for a correct diagnosis of glaucoma.

The conventional β-zone has, to date, been defined as visible sclera along with visible large choroidal vessels on fundus exam. It therefore included the (new) β-zone and the (new) γ-zone (see Sect 10.2.3). Since the new β-zone has been associated with glaucoma, whereas the γ-zone has been found to correlate with myopia rather than glaucoma, one may infer that clinical differentiation between these two zones may increase the diagnostic utility of β-zone for glaucoma [24].

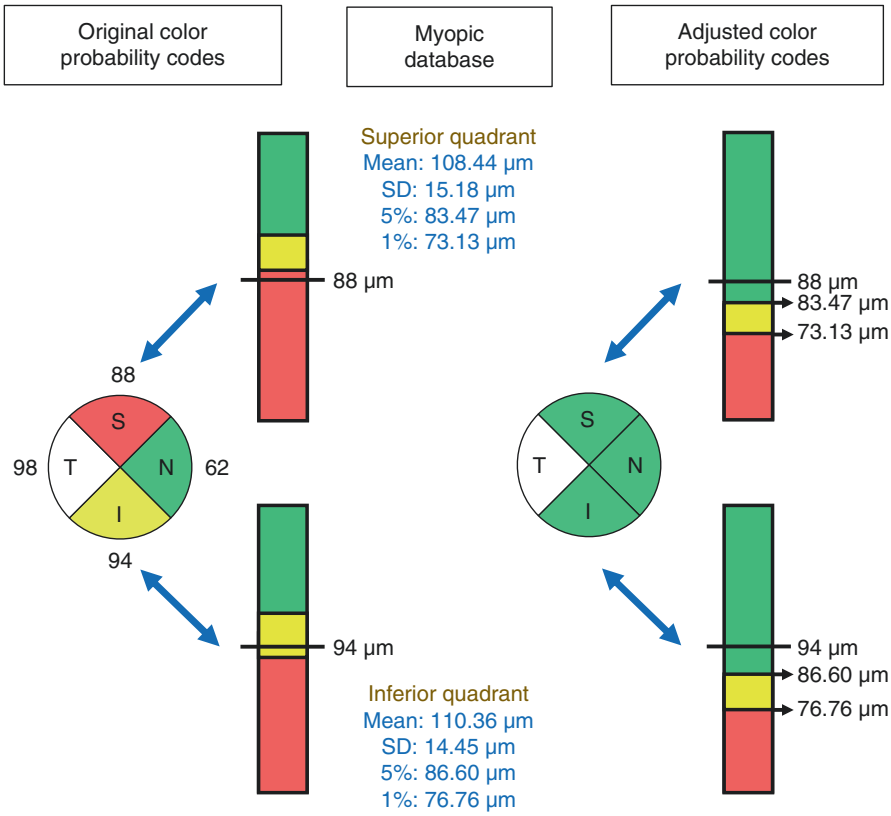

Fig. 10.11 The right eye of a 36-year-old glaucoma suspect woman with moderate myopia monitored in our clinic. Original color probability codes of retinal nerve fiber layer (RNFL) thickness display red color ($p < 1\%$) in the superior quadrant and yellow color ($1\% < p < 5\%$) in the inferior quadrant. After applying the criteria derived from the myopic database, the superior (88 µm) and inferior RNFL thickness (94 µm) are shown in green (within normal limits). For the superior quadrant, the 5% cutoff point is 83.47 µm and the 1% value is 73.13 µm. For the inferior quadrant, the 5% cutoff point is 86.60 µm and the 1% value is 76.76 µm. Adjusted color probability codes of RNFL thickness show improved color probability codes in the superior and inferior quadrants. The bar graphs indicate the percentile values of the superior and inferior quadrants for the original and adjusted color probability codes [34]

An overview of the various peripapillary zones is provided in Figs. 10.13, 10.14, 10.15 and 10.16.

In eyes with wide PPA area, the standard 3.46 mm RNFL measurement circle may include the PPA area resulting in segmentation errors. Other OCT algorithms including a larger size scan with the GMPE software of Spectralis OCT, or macular imaging may be used as complementary or alternative options (Fig. 10.17).

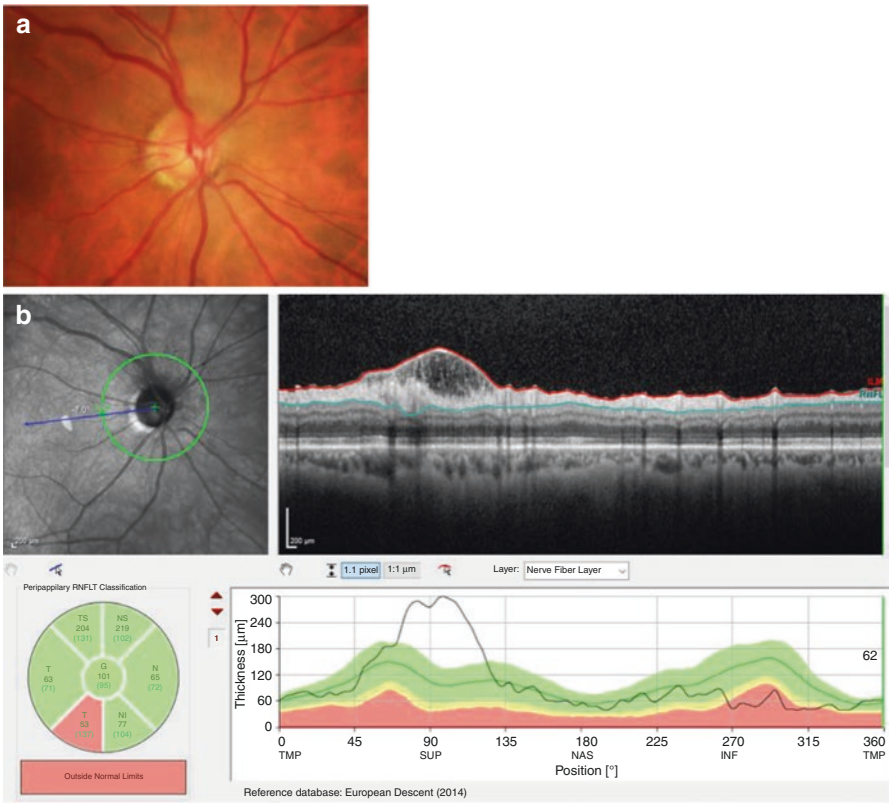

Fig. 10.12 (**a**) Disc photograph of a patient with superonasal peripapillary retinoschisis. The patient had primary open angle glaucoma and moderate myopia. (**b**) Retinal nerve fiber layer profile and thickness plot of optical coherence tomography image shows abnormal elevation of the RNFL. Note thinning of the RNFL in the temporal-inferior sector

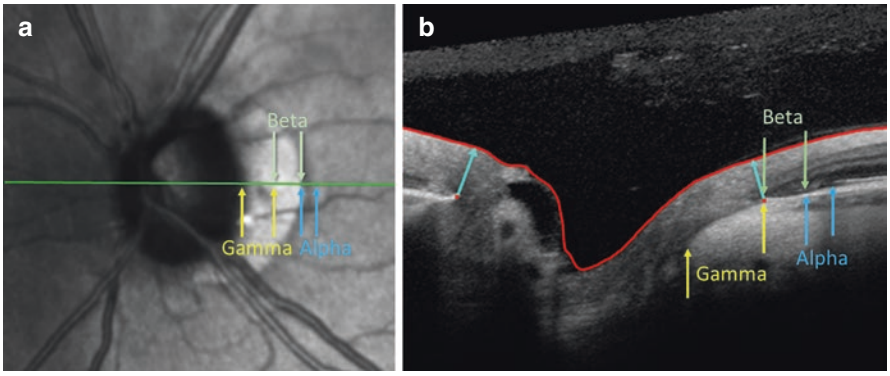

Fig. 10.13 (**a**) Peripapillary atrophy zones in the infrared image. Note that the β- and γ-zones cannot be distinguished on the IR images. (**b**) The OCT optic nerve head scan demonstrates the peripapillary α-zone (Bruch's membrane-RPE complex is present with irregularities of the retinal pigment epithelium), β-zone (Bruch's membrane present with no retinal pigment epithelium) and γ-zone (no Bruch's membrane or retinal pigment epithelium)

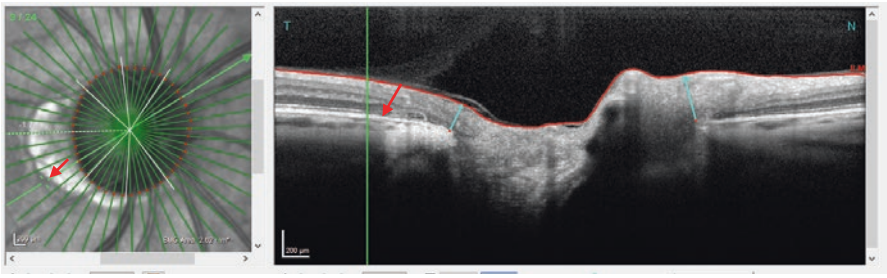

Fig. 10.14 The outer edge of the hyper-reflective area in β-zone peripapillary atrophy (PPA) corresponds to the retinal pigment epithelium ending (red arrows). Due to the temporal absence of RPE, more light can reach the underlying structures so they appear hyper-reflective on the infrared (IR) optical coherence tomography image. The Bruch's membrane ends at the same location as the choroid and the sclera. The Bruch's membrane opening is correctly identified at the inner edge of the β-zone PPA

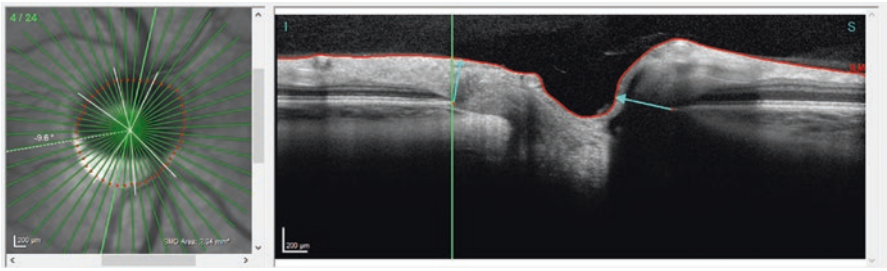

Fig. 10.15 Left, tilted optic nerve head with an infero-temporal myopic crescent (γ-zone peripapillary atrophy). As seen on the optical coherence tomography scan, the Bruch's membrane terminates before reaching the border tissue of Elschnig with significant thinning of the underlying choroid. Absence of the retinal pigment epithelium and thinned choroid enable a direct view onto the sclera seen as a white sharply demarcated zone on the infrared (IR) image. The Bruch's membrane opening is correctly detected at the outer edge of the hyper-reflectance area seen in the IR image

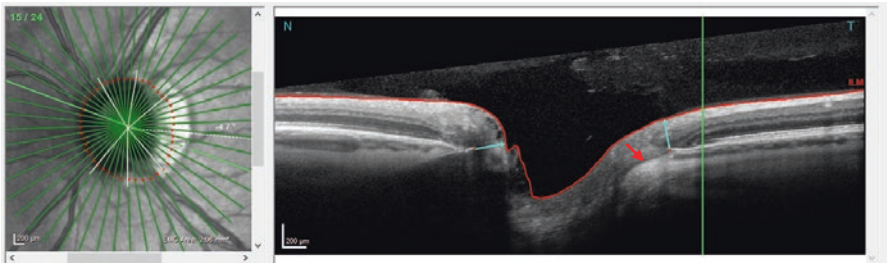

Fig. 10.16 A combination of peripapillary atrophy and temporal conus, for example in a tilted myopic disc, is possible. The outer edge of the hyper-reflective area on the infrared (IR) image corresponds to the retinal pigment epithelium (RPE) termination (green marker) while the inner edge matched an area of the border tissue of Elschnig (red arrow). The Bruch's membrane extends further than the RPE does. Therefore, the Bruch's membrane opening is located within the hyper-reflective area at the outer edge of γ-zone or rather at the inner edge of β-zone

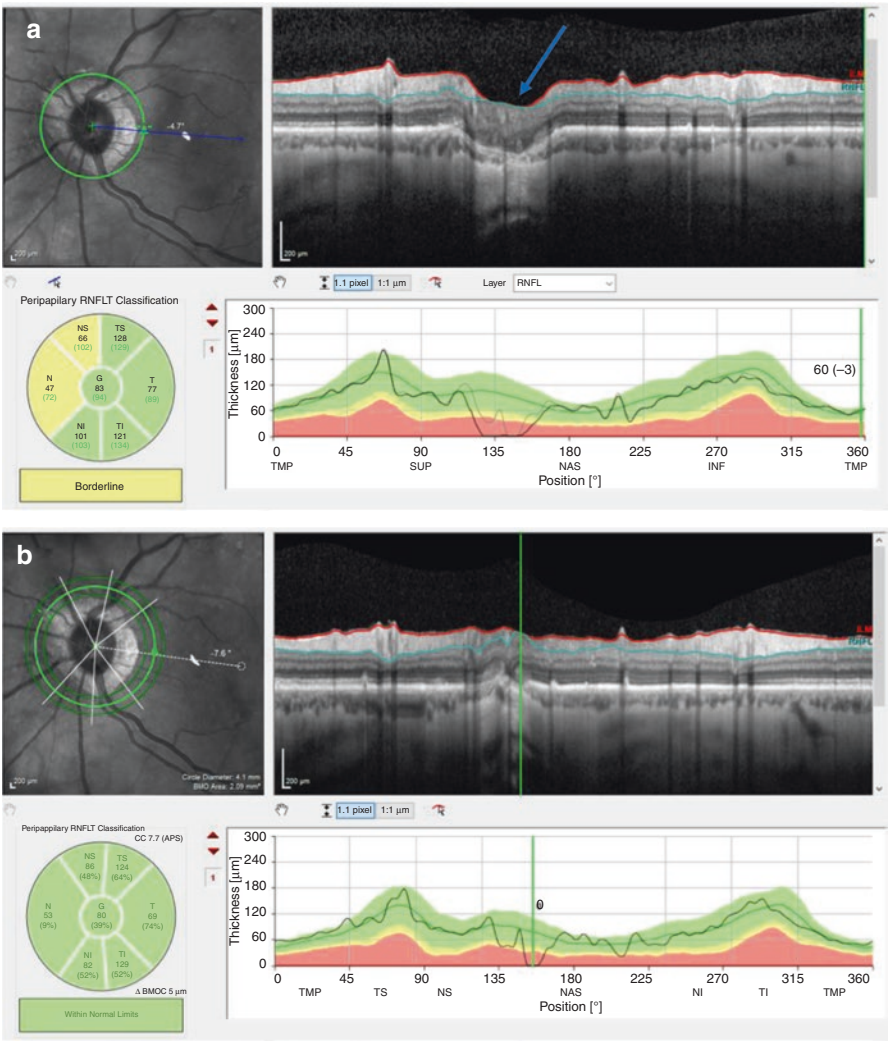

Fig. 10.17 (**a**) Peripapillary atrophy may cause localized segmentation error (blue arrow). (**b**) Changing the scan circle size to 4.1 mm decreased the extent of the area showing the segmentation error and demonstrated that the retinal nerve fiber layer (RNFL) thickness is mostly within normal limits in all the sectors. (**c**) The RNFL is within normal limits with circle scan size of 4.7 mm. (**d**) Minimum rim width analysis of the same eye revealed that neuroretinal rim thickness is within normal limits circumferentially and globally

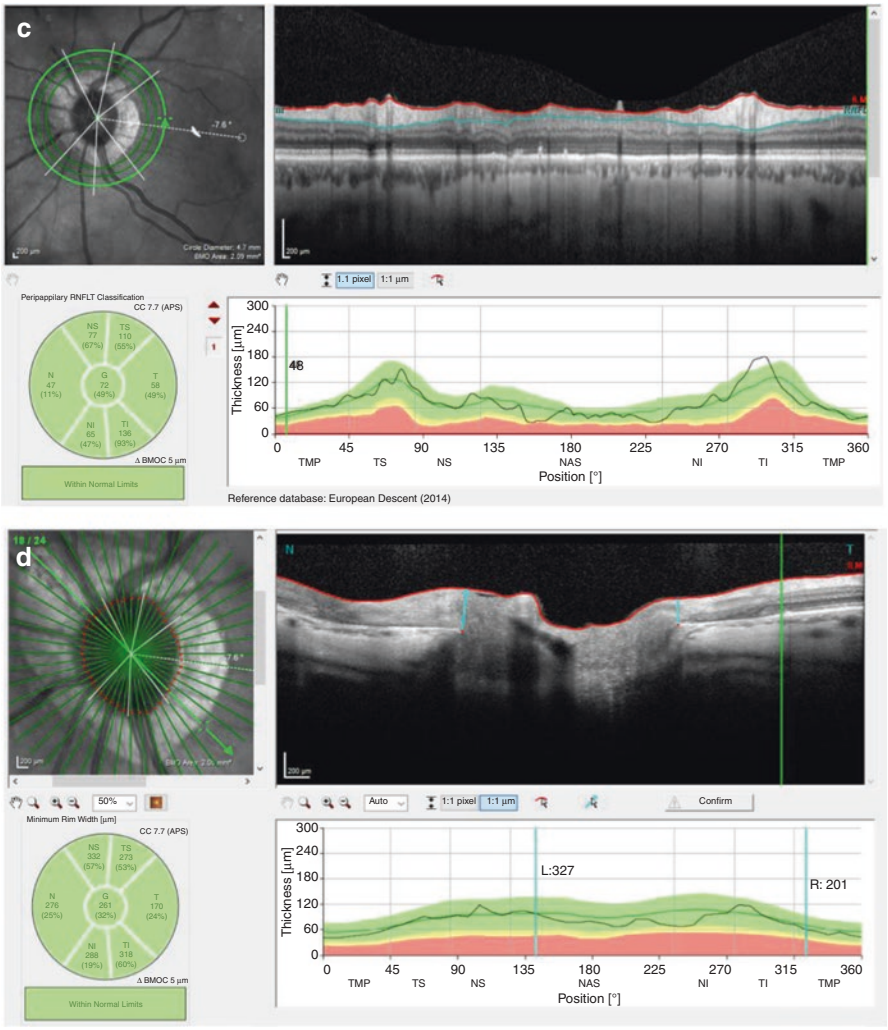

Fig. 10.17 (continued)

10.3.4 Macular Area

As the normative database of current OCT devices largely consists of data collected from normal eyes with no or low myopia, interpreting the RNFL thickness deviation maps in highly myopic eyes is commonly fraught with difficulties. Therefore, measuring the RGC cell bodies and their neural processes in the macula instead of the peripapillary axons could be a viable alternative (Fig. 10.18). The ganglion cell layer (GCL) or ganglion cell complex (GCC) can be segmented and measured in

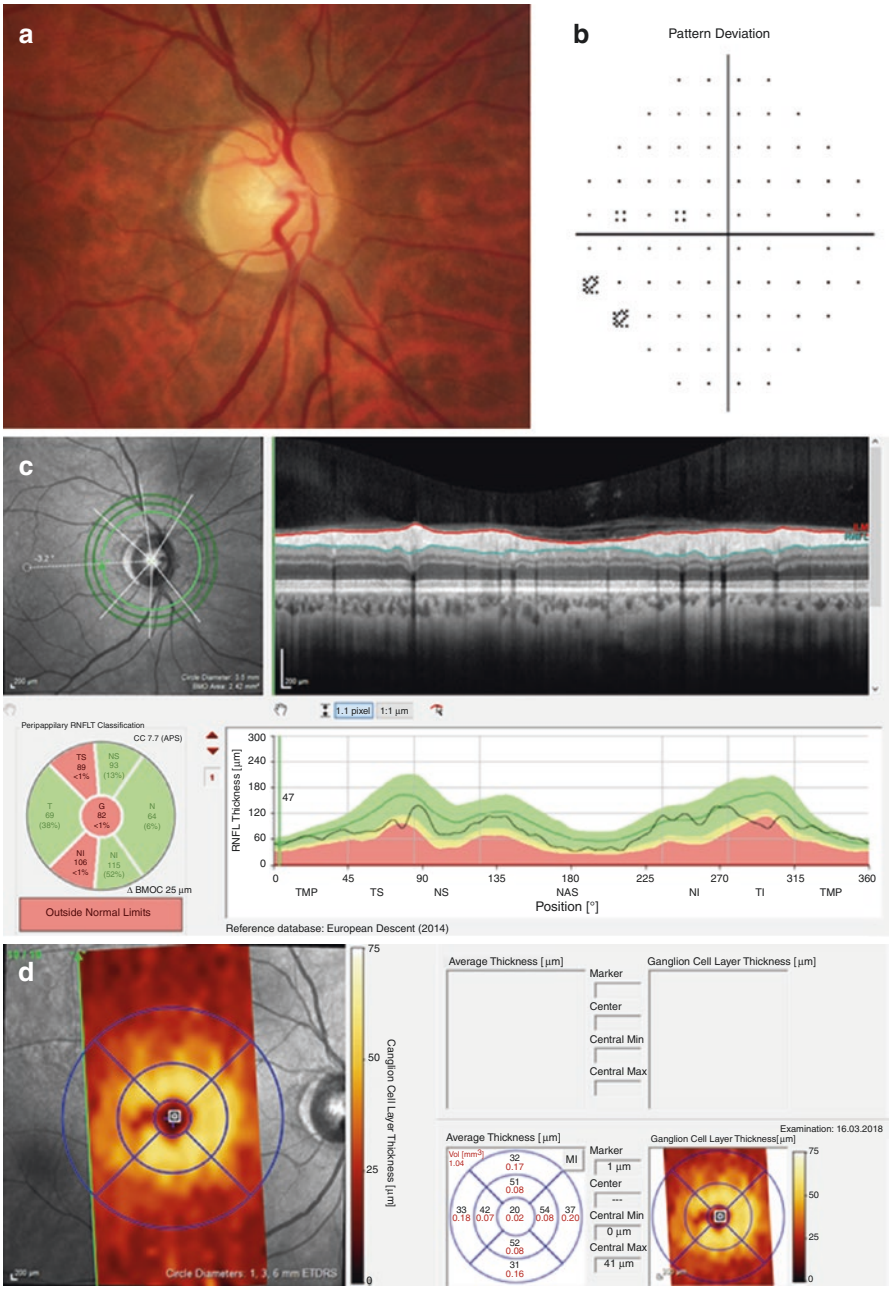

Fig. 10.18 (**a**) A young male patient with ocular hypertension and moderate myopia (−3.25 diopters spherical equivalent) in the right eye. The optic disc appeared healthy on exam. (**b**) The central 24-2 visual field test was within normal limits. (**c**) Retinal nerve fiber layer analysis showed thinning in the temporal superior and temporal inferior sectors both classified as outside normal limits. (**d**) The ganglion cell layer thickness map did not show any loss compatible with glaucoma and average thickness values on the ETDRS grid were symmetrical between the superior and inferior hemispheres. (**e**) The minimum rim width analysis results were within normal limits

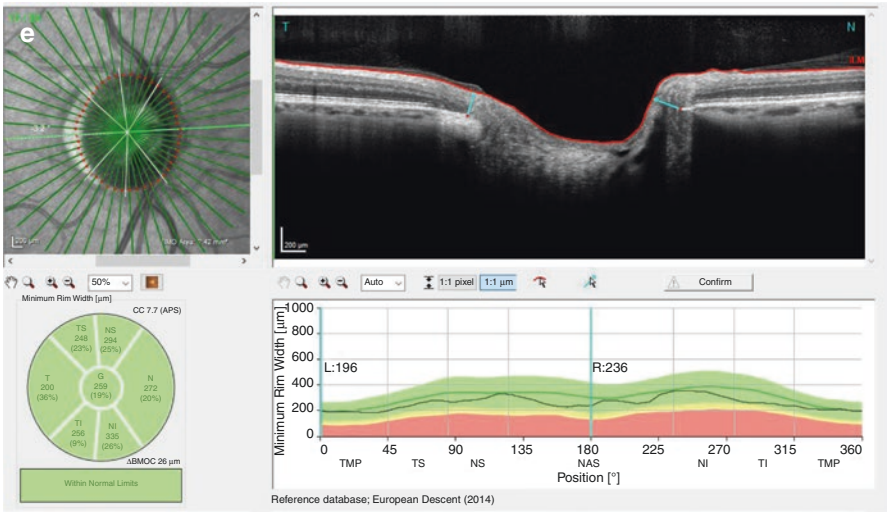

Fig. 10.18 (continued)

highly myopic eyes, but further longitudinal, large-scale studies are needed to validate its translation into clinical practice.

Several studies reported that the GCC parameters of SD-OCT attained higher diagnostic power than both ONH parameters and peripapillary RNFL measurements for detection of glaucoma concomitant with high myopia [35–37]. These studies concluded that assessment of GCC parameters is a useful technique complementary to peripapillary RNFL thickness assessment for clinically evaluating concomitant glaucoma and high myopia. Akashi and associates reported significant differences in the diagnostic performances of the peripapillary RNFL thickness measurements for detection of glaucoma in highly myopic eyes with early VF loss when highly myopic normal eyes were used as the control group compared to a non-highly myopic normal group regardless of the OCT device used [38]. Highly myopic normal eyes showed higher receiver operating characteristic curves (AUCs) for the temporal quadrant circumpapillary RNFL thickness but lower AUCs for the superior and inferior RNFL thicknesses compared with nonhighly myopic normal eyes. In contrast, when the GCC thickness was used for this purpose, the difference was not statistically significant. However, use of macular RNFL thickness led to high false positive detection rate in high myopia.

Application of a myopic normative database for ganglion cell inner plexiform layer (GCIPL) thickness has been reported to significantly improve detection of glaucoma in myopic eyes [34]. Seo and associates investigated the effect of myopia and optic disc size on the GCIPL and RNFL thickness profiles obtained with Cirrus HD-OCT. RNFL and GCIPL thickness profiles were affected by the refractive error and optic disc size. They recommend RNFL and GCIPL analysis in the evaluation of glaucoma should always be interpreted with reference to the refractive status and optic disc size [39].

10.4 Key Points

- The clinician should look for signs of segmentation errors and artifacts on the OCT images and always examine the raw images. Significant defects seen on the OCT frequently correspond with defects on the VF.
- Instead of relying on the color coding of OCT results to indicate abnormality, monitoring the RNFL and ONH parameters with OCT *over time* in myopic eyes may be helpful, since these parameters would not be expected to change in normal myopic patients but would do so in a progressive optic neuropathy such as glaucoma. In other words, the clinician should focus on comparing the patient to himself or herself rather than the general population. Examination of the RNFL raw images over time can be helpful.
- Before making a clinical decision, the family history, ethnicity, severity of myopia, central corneal thickness, corneal hysteresis, and the IOPs of the patient also need to be considered.
- The clinician should gather as much information and data as he or she can, including ONH photographs, VFs, and OCT images of the ONH (BMO-MRW), RNFL, and macula, and should put more emphasis on his or her clinical impression in myopic eyes.

References

1. Shim SH, Sung KR, Kim JM, Kim HT, Jeong J, Kim CY, Lee MY, Park KH. Korean ophthalmological society. The prevalence of open-angle glaucoma by age in myopia: the Korea National Health and nutrition examination survey. Curr Eye Res. 2017;42:65–71.
2. Chon B, Qiu M, Lin SC. Myopia and glaucoma in the south Korean population. Invest Ophthalmol Vis Sci. 2013;54:6570–7.
3. Mitchell P, Hourihan F, Sandbach J, Wang JJ. The relationship between glaucoma and myopia: the blue mountains eye study. Ophthalmology. 1999;106:2010–5.
4. Xu L, Li Y, Wang S, Wang Y, Wang Y, Jonas JB. Characteristics of highly myopic eyes: the Beijing eye study. Ophthalmology. 2007;114:121–6.
5. Melo GB, Libera RD, Barbosa AS, Pereira LM, Doi LM, Melo LA Jr. Comparison of optic disk and retinal nerve fiber layer thickness in nonglaucomatous and glaucomatous patients with high myopia. Am J Ophthalmol. 2006;142:858–60.
6. You QS, Peng XY, Xu L, Chen CX, Wang YX, Jonas JB. Myopic maculopathy imaged by optical coherence tomography: the Beijing eye study. Ophthalmology. 2014;121:220–4.
7. Leung CK, Mohamed S, Leung KS, Cheung CY, Chan SL, Cheng DK, Lee AK, Leung GY, Rao SK, Lam DS. Retinal nerve fiber layer measurements in myopia: an optical coherence tomography study. Invest Ophthalmol Vis Sci. 2006;47:5171–6.
8. Wong YZ, Lam AK. The roles of cornea and axial length in corneal hysteresis among emmetropes and high myopes: a pilot study. Curr Eye Res. 2015;40:282–9.
9. Jiang Z, Shen M, Mao G, Chen D, Wang J, Qu J, Lu F. Association between corneal biomechanical properties and myopia in Chinese subjects. Eye (Lond). 2011;25:1083–9.
10. Shen M, Fan F, Xue A, Wang J, Zhou X, Lu F. Biomechanical properties of the cornea in high myopia. Vis Res. 2008;48:2167–71.
11. Kim TW, Kim M, Weinreb RN, Woo SJ, Park KH, Hwang JM. Optic disc change with incipient myopia of childhood. Ophthalmology. 2012;119:21–6.

12. Jonas JB, Gusek GC, Naumann GO. Optic disk morphometry in high myopia. Graefes Arch Clin Exp Ophthalmol. 1988;226:587–90.
13. Witmer MT, Margo CE, Drucker M. Tilted optic disks. Surv Ophthalmol. 2010;55:403–28.
14. Jonas JB, Xu L. Histological changes of high axial myopia. Eye (Lond). 2014;28:113–7.
15. Morgan WH, Yu DY, Alder VA, Cringle SJ, Cooper RL, House PH, Constable IJ. The correlation between cerebrospinal fluid pressure and retrolaminar tissue pressure. Invest Ophthalmol Vis Sci. 1998;39:1419–28.
16. Tezel G, Trinkaus K, Wax MB. Alterations in the morphology of lamina cribrosa pores in glaucomatous eyes. Br J Ophthalmol. 2004;88:251–6.
17. Tay E, Seah SK, Chan SP, Lim AT, Chew SJ, Foster PJ, Aung T. Optic disk ovality as an index of tilt and its relationship to myopia and perimetry. Am J Ophthalmol. 2005;139:247–52.
18. Jonas JB. Optic disk size correlated with refractive error. Am J Ophthalmol. 2005;139:346–8.
19. Jonas JB, Nguyen XN, Gusek GC, Naumann GO. Parapapillary chorioretinal atrophy in normal and glaucoma eyes. I. Morphometric data. Invest Ophthalmol Vis Sci. 1989;30:908–18.
20. Jonas JB, Budde WM, Panda-Jones S. Ophthalmoscopic evaluation of the optic nerve head. Surv Ophthalmol. 1999;43:293–320.
21. Jonas JB, Jonas SB, Jonas RA, Holbach L, Dai Y, Sun X, Panda-Jonas S. Parapapillary atrophy: histological gamma zone and delta zone. PLoS One. 2012;7(10):e47237.
22. Dichtl A, Jonas JB, Naumann GO. Histomorphometry of the optic disc in highly myopic eyes with absolute secondary angle closure glaucoma. Br J Ophthalmol. 1998;82:286–9.
23. Fantes FE, Anderson DR. Clinical histologic correlation of human peripapillary anatomy. Ophthalmology. 1989;96:20–5.
24. Dai Y, Jonas JB, Huang H, Wang M, Sun X. Microstructure of parapapillary atrophy: beta zone and gamma zone. Invest Ophthalmol Vis Sci. 2013;54:2013–8.
25. Ng DS, Cheung CY, Luk FO, Mohamed S, Brelen ME, Yam JC, Tsang CW, Lai TY. Advances of optical coherence tomography in myopia and pathologic myopia. Eye (Lond). 2016;30:901–16.
26. Hosseini H, Nassiri N, Azarbod P, Giaconi J, Chou T, Caprioli J, Nouri-Mahdavi K. Measurement of the optic disc vertical tilt angle with spectral-domain optical coherence tomography and influencing factors. Am J Ophthalmol. 2013;156:737–44.
27. Kimura Y, Akagi T, Hangai M, Takayama K, Hasegawa T, Suda K, Yoshikawa M, Yamada H, Nakanishi H, Unoki N, Ikeda HO, Yoshimura N. Lamina cribrosa defects and optic disc morphology in primary open angle glaucoma with high myopia. PLoS One. 2014;9(12):e115313. https://doi.org/10.1371/journal.pone.0115313. eCollection 2014
28. Kang SH, Hong SW, Im SK, Lee SH, Ahn MD. Effect of myopia on the thickness of the retinal nerve fiber layer measured by cirrus HD optical coherence tomography. Invest Ophthalmol Vis Sci. 2010;51:4075–83.
29. Lee KH, Kim CY, Kim NR. Variations of retinal nerve fiber layer thickness and ganglion cell-inner plexiform layer thickness according to the torsion direction of optic disc. Invest Ophthalmol Vis Sci. 2014;55:1048–55.
30. Bae SH, Kang SH, Feng CS, Park J, Jeong JH, Yi K. Influence of myopia on size of optic nerve head and retinal nerve fiber layer thickness measured by spectral domain optical coherence tomography. Korean J Ophthalmol. 2016;30:335–43.
31. Budenz DL, Anderson DR, Varma R, Schuman J, Cantor L, Savell J, Greenfield DS, Patella VM, Quigley HA, Tielsch J. Determinants of normal retinal nerve fiber layer thickness measured by stratus OCT. Ophthalmology. 2007;114:1046–52.
32. Nowroozizadeh S, Cirineo N, Amini N, Knipping S, Chang T, Chou T, Caprioli J, Nouri-Mahdavi K. Influence of correction of ocular magnification on spectral-domain OCT retinal nerve fiber layer measurement variability and performance. Invest Ophthalmol Vis Sci. 2014;55:3439–46.
33. Savini G, Barboni P, Parisi V, Carbonelli M. The influence of axial length on retinal nerve fibre layer thickness and optic-disc size measurements by spectral-domain OCT. Br J Ophthalmol. 2012;96:57–61.
34. Seol BR, Kim DM, Park KH, Jeoung JW. Assessment of optical coherence tomography color probability codes in myopic glaucoma eyes after applying a myopic normative database. Am J Ophthalmol. 2017;183:147–55.

35. Zhang C, Tatham AJ, Weinreb RN, Zangwill LM, Yang Z, Zhang JZ, Medeiros FA. Relationship between ganglion cell layer thickness and estimated retinal ganglion cell counts in the glaucomatous macula. Ophthalmology. 2014;121:2371–9.
36. Shoji T, Sato H, Ishida M, Takeuchi M, Chihara E. Assessment of glaucomatous changes in subjects with high myopia using spectral domain optical coherence tomography. Invest Ophthalmol Vis Sci. 2011;52:1098–102.
37. Kim NR, Lee ES, Seong GJ, Kang SY, Kim JH, Hong S, Kim CY. Comparing the ganglion cell complex and retinal nerve fibre layer measurements by Fourier domain OCT to detect glaucoma in high myopia. Br J Ophthalmol. 2011;95:1115–21.
38. Akashi A, Kanamori A, Ueda K, Inoue Y, Yamada Y, Nakamura M. The ability of SD-OCT to differentiate early glaucoma with high myopia from highly myopic controls and nonhighly myopic controls. Invest Ophthalmol Vis Sci. 2015;56:6573–80.
39. Seo S, Lee CE, Jeong JH, Park KH, Kim DM, Jeoung JW. Ganglion cell-inner plexiform layer and retinal nerve fiber layer thickness according to myopia and optic disc area: a quantitative and three-dimensional analysis. BMC Ophthalmol. 2017;17:22. https://doi.org/10.1186/s12886-017-0419-1.